J Solid State Electrochem (2012) 16:2699–2708
DOI 10.1007/s10008-012-1697-4

ORIGINAL PAPER

Electrocatalytic oxidation of methanol onto platinum particles decorated nanostructured poly (1,5-diaminonaphthalene) film

Jahan Bakhsh Raoof · Reza Ojani · Sayed Reza Hosseini

Received: 9 November 2011 / Revised: 13 February 2012 / Accepted: 15 February 2012 / Published online: 1 March 2012

Abstract In this work, platinum particles decorated nanostructured poly (1,5-diaminonaphthalene) modified glassy carbon electrode (Pt/Nano-PDAN/MGCE) is prepared. The composite catalysts are characterized by scanning electron microscopy, energy dispersive spectroscopy, and electrochemical methods. The electrochemical methanol oxidation reaction is studied at the surface of this modified electrode. At same Pt loading, the Pt/Nano-PDAN/MGCE can act as higher efficient catalyst for methanol oxidation than that Pt/MGCE. Then, the influence of some parameters such as potential scan rates, switching potential, and methanol concentration on its oxidation as well as long-term stability of the modified electrode have studied by electrochemical methods. Also, ability of the modified electrode toward electrocatalytic oxidation of formaldehyde as an intermediate in methanol oxidation has been investigated.

Keywords Nanostructured poly (1,5-diaminonaphthalene) film · Platinum particles · Methanol · Electrocatalytic oxidation · Formaldehyde

Introduction

The electrocatalytic oxidation of methanol is a hot topic due to its relevance in the operation of direct methanol fuel cells. However, commercialization of these fuel cells has been facing serious difficulties due to kinetic constraints of the electrochemical methanol oxidation reaction [1–4]. Although non-noble metals catalysts have been investigated and used for methanol electrooxidation [5–7], Pt and its alloys are one of the best electrocatalysts for use towards the methanol oxidation. In order to enhance the electrocatalytic activity of anode catalyst in methanol oxidation, the use of Pt seems inevitable, but its price is high and it increases the anode cost. An effective way to decrease the anodes cost is lowering the amount of Pt by making high dispersed Pt particles on carbon supports [8–10]. Carbon materials are of special interest due to their outstanding properties, such as their tunable shape, size, porosity, corrosion resistance, chemical stability, low cost, electrical conductivity, and good thermal resistance. The combination of all these characteristics has promoted the use of these materials as electrode supports.

It is well known that conducting polymers (CPs) with porous structures and high surface areas have been proved to be suitable host materials for dispersion of Pt particles [11–14]. The reason for the incorporation of Pt particles into the porous matrixes is to increase the specific surface areas of them and thus improve their electrocatalytic activity. Another reason is higher tolerance of the Pt particles to poisoning effect due to adsorption of CO species, in comparison with serious problem of poisoning effect on bulk Pt electrodes. The composites of CPs with Pt particles permit a facile flow of electronic charges through the polymer matrix during electrochemical processes. However, the studies of CPs as supports of Pt particles were centered on polyaniline, polypyrrole, polythiophene, and their derivatives [15–17]. Therefore, it would be quite interesting to extend such studies to other CPs which might be suitable materials for the catalyst particles.

Recently, we have reported nickel/poly (1,5-diaminonaphthalene)-modified carbon paste electrode for electrocatalytic oxidation of methanol and formaldehyde in alkaline medium [18, 19]. Our literature survey indicates that there is no report

J. B. Raoof (✉) · R. Ojani · S. R. Hosseini
Department of Analytical Chemistry, Faculty of Chemistry,
University of Mazandaran,
3rd Kilometer of Air Force Road,
47416-95447 Babolsar, Iran
e-mail: j.raoof@umz.ac.ir

on the electrochemical oxidation of methanol and formaldehyde onto Pt particles decorated nanostructured poly (1,5-diaminonaphthalene) modified glassy carbon electrode (Pt/Nano-PDAN/MGCE). Indeed, it is remarkable and important to investigate new supports for the synthesis of nanomaterials as potent catalyst for fuel cell applications. In this way, the use of conducting polymer as 1,5-diaminonaphthalene (DAN) for enhanced the activity of Pt particles is very interesting. Therefore, in the this work, in order to investigate the effect of poly (1,5-diaminonaphthalene) film towards the electrooxidation of the small organic molecules, Pt/MGCE and Pt/Nano-PDAN/MGCE were fabricated and characterized by scanning electron microscopy (SEM), energy dispersive spectroscopy (EDS) and electrochemical methods. It has also described how nano-PDAN improves the electrocatalytic efficiency of Pt particles towards electrooxidation of methanol and formaldehyde which have significant attractions in fuel cells technology.

Experimental

Materials

The solvent used in this work was distilled water. Sulfuric acid (from Fluka) was used as supporting electrolyte. The DAN monomer was purchased from Merck. Formaldehyde and $H_2PtCl_6{\cdot}6H_2O$ from Merck were used as received. Methanol (from Merck) used in this work was analytical grade.

Instrumentation

Electrochemical experiments were performed using AUTOLAB PGSTAT 30 electrochemical analysis system and GPES 4.9 software package (Eco Chemie, Netherlands). The utilized three-electrode system was composed of saturated calomel electrode (SCE) as reference electrode, Pt wire as auxiliary electrode, and GCE (1.5 mm in diameter, Azar electrode Co., Iran) as working electrode substrate. The surface morphology and elemental composition of the deposits were evaluated by scanning electron microscope (model VEGA-Tescan, Razi Metallurgical Research Center) equipped with an energy dispersive spectrometer (EDS). All potentials reported in this work referred to the SCE.

The electrode modification

Prior to the modification of GCE, it was polished with alumina slurries on a polishing cloth to a mirror finish and then ultrasonically cleaned for 2.0 min in ethanol. Then, the electrode was rinsed thoroughly with distilled water. The Pt particles decorated PDAN/MGCE was prepared in two steps: (a) electrochemical polymerization of DAN monomer by using potential cycling (seven cycles between −0.2 and 0.9 V at υ= 100 mV s^{-1}) in aqueous solution containing 0.5 M H_2SO_4 and 1.0 mM DAN for preparation of PDAN film; (b) the PDAN-modified GCE was soaked in a freshly prepared 2.0 mM H_2PtCl_6+0.5 M H_2SO_4 solution for 15.0 min to let metal ions fully adsorb into the PDAN, then the electrodeposition of the Pt particles were performed at constant potential of −0.2 V vs. SCE for fabrication of Pt/PDAN/MGCE. The amount of Pt particles loaded (m/μg=0.5 Q_{net}) onto the PDAN/MGCE was estimated from the integral of current–time transient response (Q_{net}/mC) during the deposition process by assuming that the reduction efficiency of Pt (IV)–Pt (0) is 100% [20–22]. The Q_{net} (net charge) consumed for deposition can be calculated

Table 1 Surface parameters of Pt deposited on the GCE

Surface parameters	Pt/MGCE	Pt/Nano-PDAN/MGCE
Pt loading/μg cm^{-2}	150	150
A_r/cm^2	0.40	0.47
RF	22.2	26.1
Specific surface area, S/m^2 g^{-1}	14.8	17.4
Geometric area, A_g/cm^2	0.018	0.018

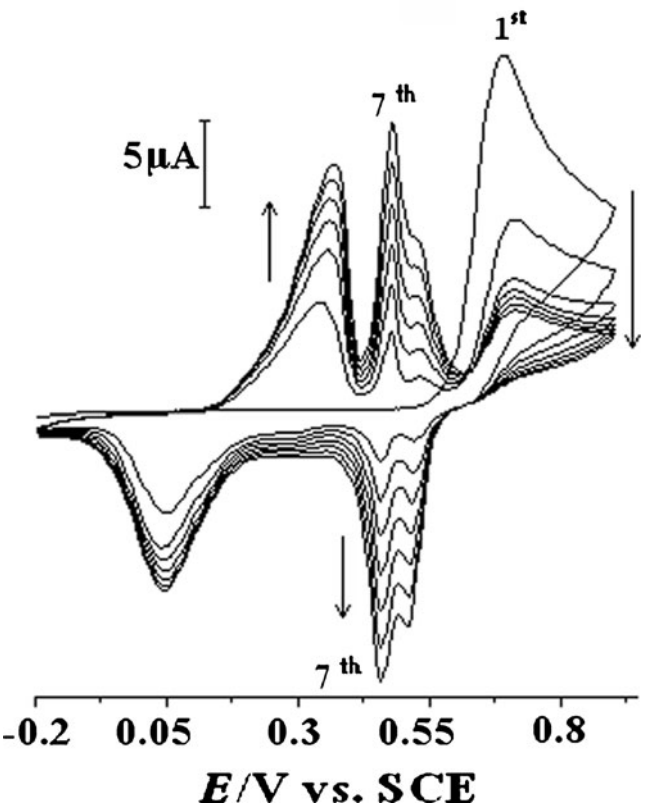

Fig. 1 Electropolymerization of DAN in 1.0 mM monomer+0.5 M H_2SO_4 solution onto GCE. The *arrows* indicate the currents trend during the cyclic voltammetry at υ=0.1 V s^{-1}

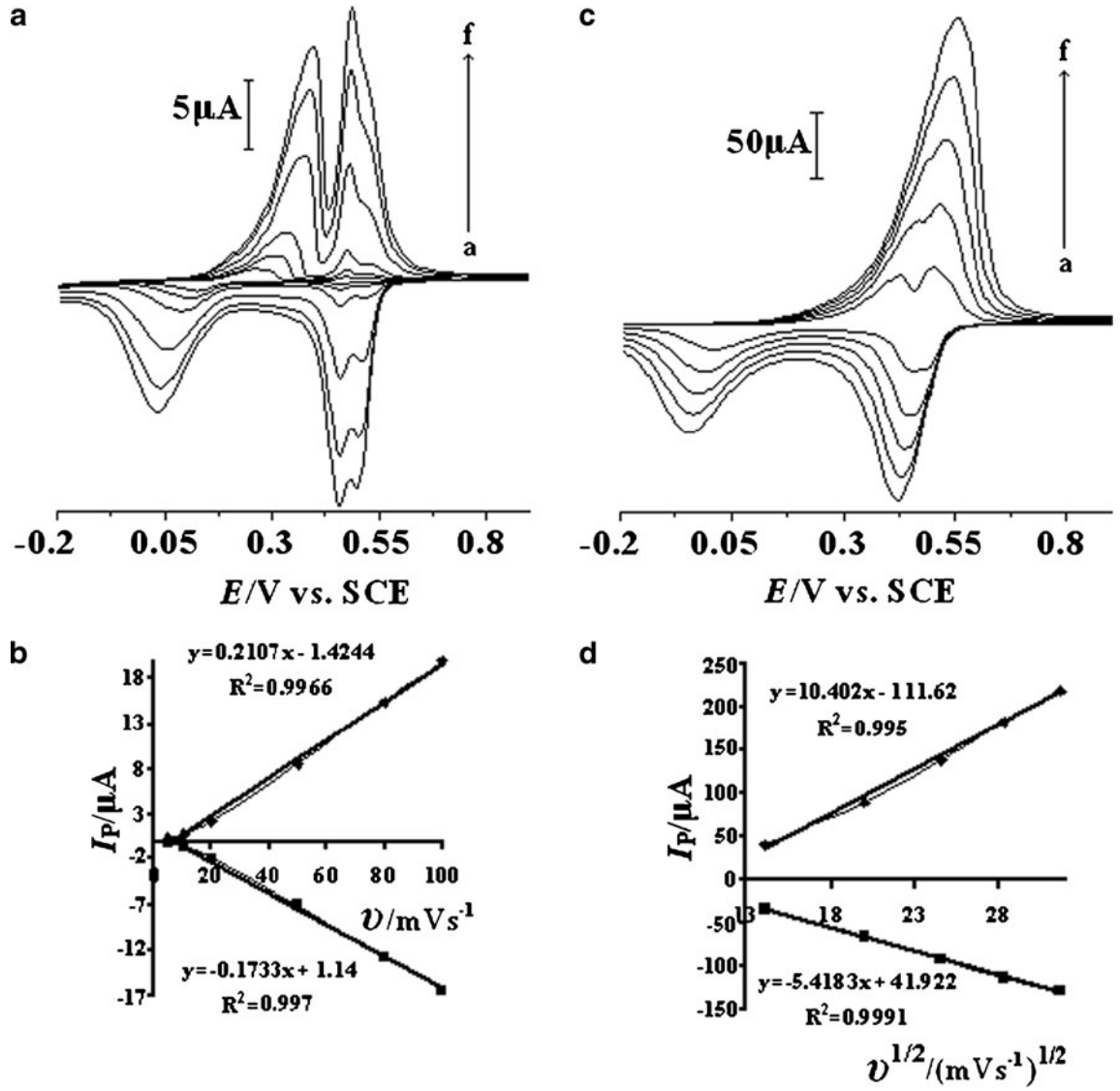

Fig. 2 Cyclic voltammograms of the PDAN/MGCE in 0.5 M H_2SO_4 solution; **a** at lower values of υ: *a* 0.005 Vs^{-1}, *b* 0.01 Vs^{-1}, *c* 0.02 Vs^{-1}, *d* 0.05 Vs^{-1}, *e* 0.08 Vs^{-1}, and *f* 0.10 Vs^{-1} and **c** at higher values of υ: *a* 0.20 Vs^{-1}, *b* 0.40 Vs^{-1}, *c* 0.60 Vs^{-1}, *d* 0.80 Vs^{-1}, and *f* 1.0 Vs^{-1}. The dependency of peak currents on the υ (**b**) and on the $\upsilon^{1/2}$ (**d**)

by subtraction of charges obtained from chronoamperogram of 2.0 mM H_2PtCl_6 solution and blank solution. In this work, the amount of deposited Pt was controlled about 2.7 μg which corresponds to a charge of 0.3 C/cm^2. The real surface area (A_r) of the Pt catalysts can be estimated from the integrated charge in the hydrogen adsorption/desorption region of the cyclic voltammogram. Similarly, the roughness factor (RF) can be estimated by dividing A_r to geometric area, A_g, of the electrode. Table 1 summarizes the surface parameters for the different modified electrodes. After Pt particles deposition, the electrode was rinsed with distilled water. At beginning of experiments, the electrodes were immersed in 0.5 M H_2SO_4 solution and potentials were cycled between −0.25 to 1.3 V at υ=0.05 Vs^{-1} until repeatable cyclic voltammograms were attained. All experiments were carried out at ambient temperature.

Results and discussion

Electrochemical polymerization

Figure 1 shows the typical multi-sweep cyclic voltammograms during the electropolymerization of DAN monomer in 0.5 M H_2SO_4 solution. As can be seen in this figure, in the first anodic sweep, the oxidation of DAN occurs as a distinct irreversible anodic peak (E_p=0.7 V), corresponding to the oxidation process of monomer amine groups into their cationic radicals. A part of the oxidation products is deposited on the electrode, as a poly (1,5-diaminonaphthalene) film. With consecutive potential cycling, the monomer oxidation peak current decreases and several redox peaks (at about 0.52, 0.54, 0.46, 0.48, 0.05, and 0.36 V) appear due to

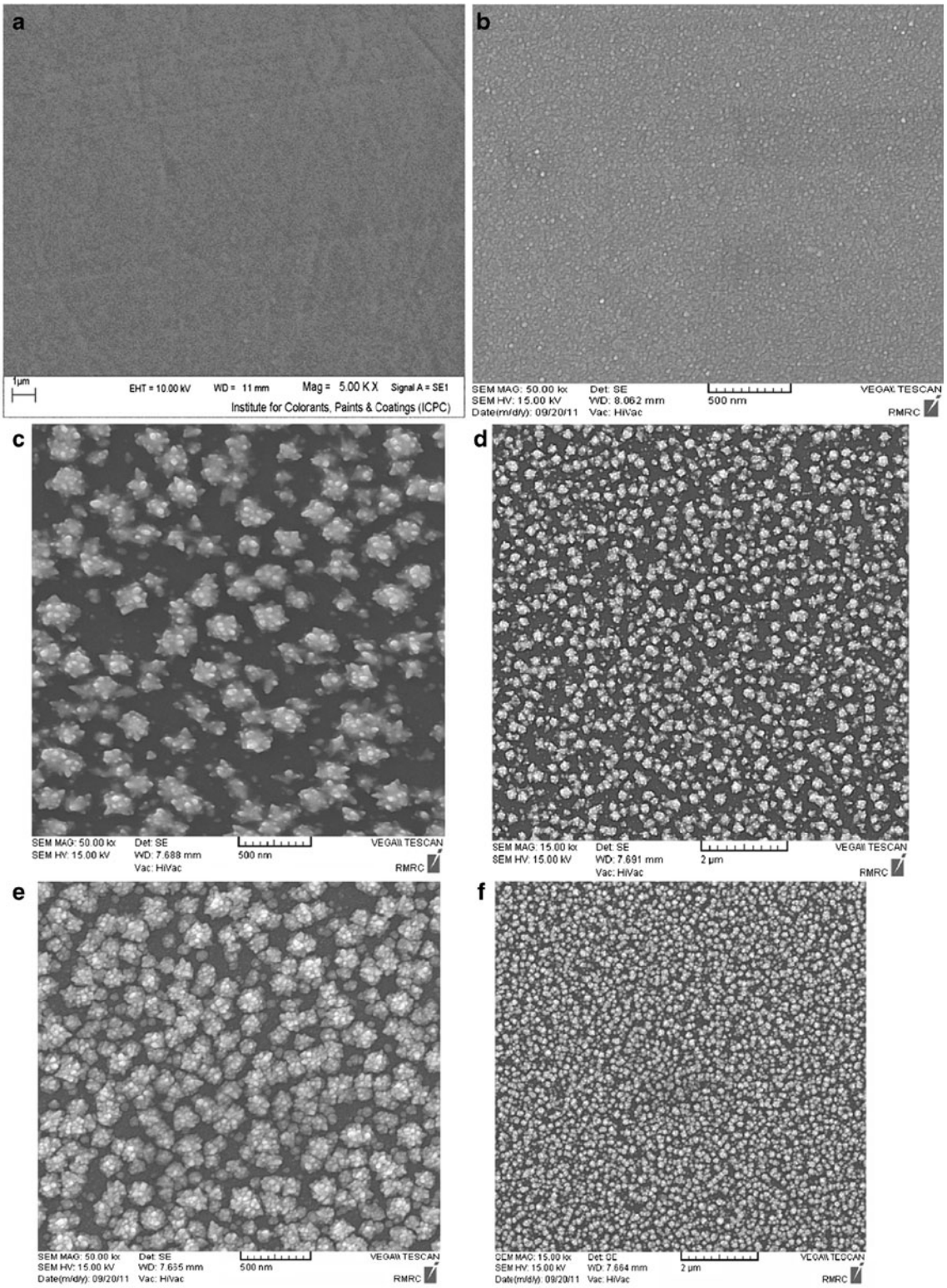

Fig. 3 SEM images of bare GCE (**a**), Nano-PDAN/MGCE (**b**), Pt/MGCE (**c**, **d**), and Pt/Nano-PDAN/MGCE (**e**, **f**)

the polymer film formation. Also, the polymer peak currents increase with increasing of potential cycles [23, 24]. In fact, in the successive cycles, the shape of the voltammograms becomes more complicated. The changes in the shape may be attributed to the soluble oxidation products that can be adsorb and/or react on the electrode surface. The decreasing of monomer oxidation current is due to less surface activity when covered with newly formed polymer film.

Cyclic voltammetry behavior of the PDAN/MGCE

The electrochemical properties of the PDAN were investigated by cyclic voltammetry in 0.5 M H_2SO_4 solution. Stability of the prepared film was also checked with cyclic voltammetry, which showed the peak currents almost remain constant. This indicates that PDAN has good stability in H_2SO_4 solution. Furthermore, this film is hard to remove from the GCE surface. The only way to remove the film is to polish the electrode surface mechanically, indicating a mechanical stability. Figure 2 represents cyclic voltammograms of the PDAN/MGCE at different potential sweep rates (υ). Peak-to-peak potential separation is deviated from the theoretical value of zero and increases at higher potential sweep rates. As shown, the peak currents increase with increasing of υ and are proportional to υ at $\upsilon \leq 0.1\ Vs^{-1}$ (Fig. 2a, b), which indicates a surface-confined redox process [25]. In the higher range of υ ($\upsilon > 0.1\ Vs^{-1}$, Fig. 2c, d), the peak currents depend on $\upsilon^{1/2}$, signifying the dominance of a diffusion process as the rate limiting step in total redox transition of the film [26–30].

The surface morphology and elemental composition

Figure 3a shows the morphology of a bare GCE after cleaning process. As can be seen in this image, there are some defects on the surface obtain during the electrode polishing. The SEM image of PDAN shows nanostructured film consisting of small particles less than 100 nm and the surface is homogenously covered with them (Fig. 3b). The structure of this matrix is beneficial to disperse Pt particles because formation of the polymer film onto GCE significantly reduces its defects to make a smooth and uniform surface as nucleation centers for the formation of metal atoms. It yields large available area and, in the case of introducing of Pt particles, with better dispersion and/or distribution. Images (Fig. 3c, d) show the morphologies of the same Pt/MGCE at different magnifications. As can be seen, the large spherical aggregates may be formed through the settlement of several small Pt particles. Only abundant conjugated Pt particles with diameter of 0.2 μm were electrodeposited onto the bare clean GCE. Images (Fig. 3e, f) show the morphologies of the Pt/Nano-PDAN/MGCE at different magnifications. Agglomerated particles (average size, 130 nm) with higher effective surface area were uniformly distributed on the electrode surface. The polymeric structure prevents the Pt particles agglomerating and coalescing during the electrodeposition and also stabilizes them on the electrode surface. Furthermore, the microscopy demonstrates that the Pt particles were located outside (external surface) of the polymer film. These results are in agreement with electrochemical experiments.

A typical EDS spectrum for determination of the composite catalyst composition was presented in Fig. 4. From the EDS results, Pt is the major element. C is derived from GCE or PDAN film. Electrochemical evidence for the available Pt deposit was also obtained by potential cycling the Pt/Nano-PDAN/MGCE in H_2SO_4 solution in the hydrogen adsorption/desorption region.

Cyclic voltammetry of the Pt/MGCE and Pt/Nano-PDAN/MGCE

After depositing Pt particles, cyclic voltammetry of the electrodes were performed in 0.5 M H_2SO_4 solution and the electrodes showed typical hydrogen adsorption/desorption

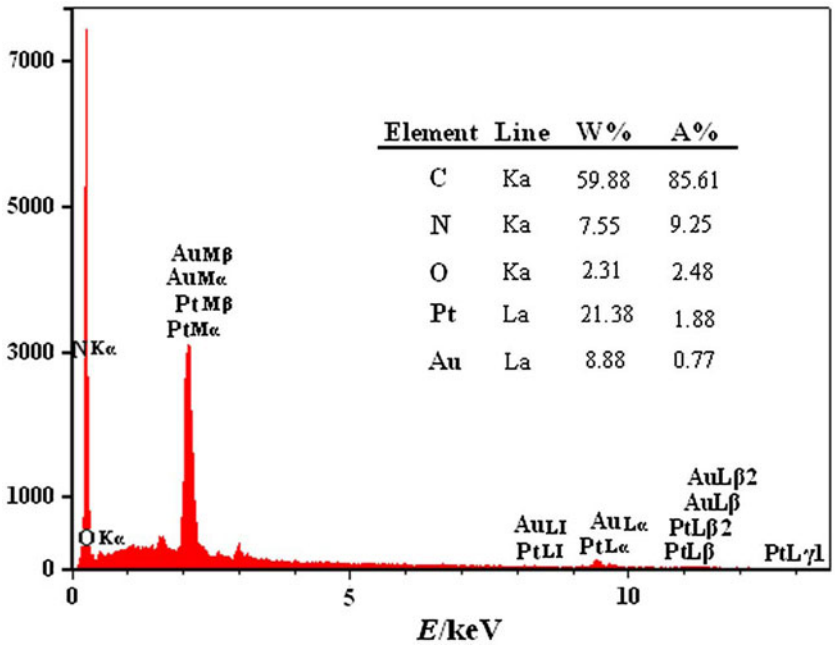

Fig. 4 EDS spectrum of the Pt/Nano-PDAN. Elemental analysis data of the modified electrode

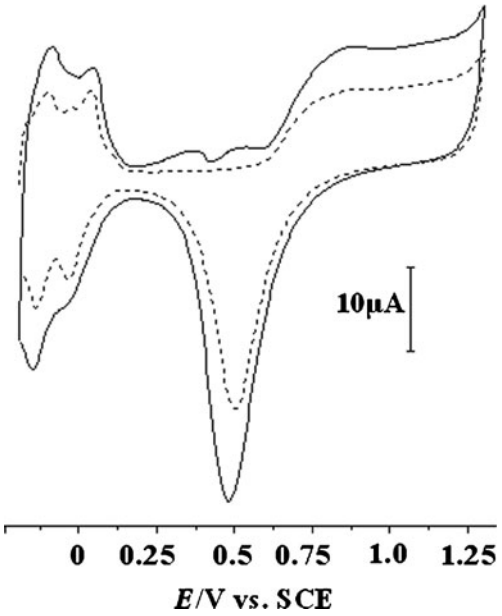

Fig. 5 Cyclic voltammograms of the Pt/MGCE (*dotted line*) and Pt/Nano-PDAN/MGCE (*solid line*) in 0.5 M H_2SO_4 solution at υ=0.05 Vs^{-1}

peaks (Fig. 5). Also, the two peaks at about 0.38 and 0.48 V are ascribable to the electrochemical response of the polymer film. It should be noted that the reduction peak of the polymer superimposed on the reduction peak of Pt oxide. The characteristic peaks (Pt–H redox peaks) in the negative region are attributed to the atomic hydrogen adsorption on Pt surface, and charge under the peaks can reflect the specific surface area of the Pt particles. Larger peaks are

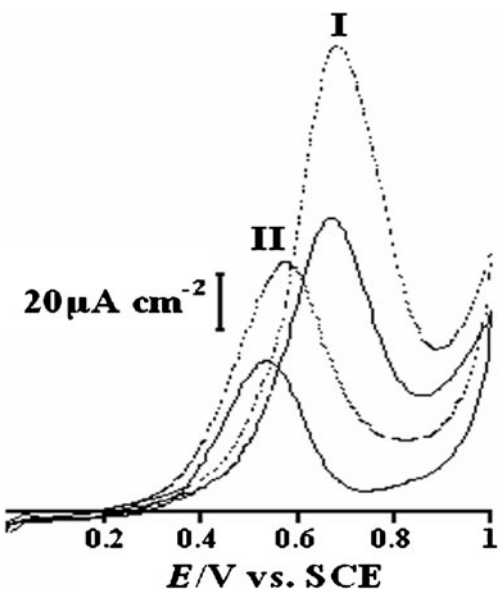

Fig. 6 Electrochemical responses of the Pt/Nano-PDAN/MGCE (*dotted line*) and Pt/MGCE (*solid line*) in 2.4 M CH_3OH+0.5 M H_2SO_4 solution at υ=0.05 Vs^{-1}

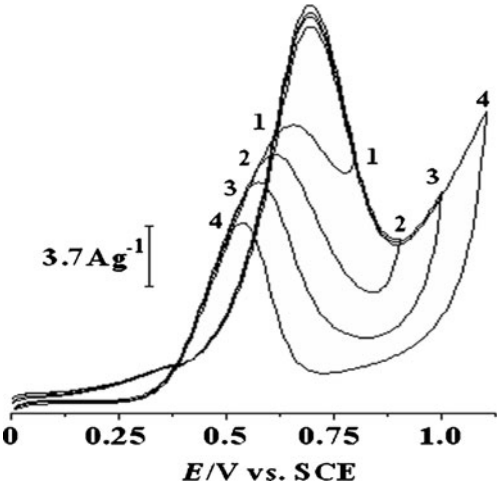

Fig. 7 Effect of upper limit potential scanning on the oxidation of 1.8 M methanol onto Pt/Nano-PDAN/MGCE in 0.5 M H_2SO_4 solution at υ=0.05 Vs^{-1}. (*1*) 0.0–0.8 V, (*2*) 0.0–0.9 V, (*3*) 0.0–1.0 V, and (*4*) 0.0–1.1 V

observed on the Pt/Nano-PDAN, reflecting high surface area of the Pt particles. According to Table 1, it is concluded that larger Pt surface is available at the Pt/Nano-PDAN/MGCE than that at Pt/MGCE. So, such Pt particles enhance the active sites towards the electrochemical oxidation of methanol and formaldehyde.

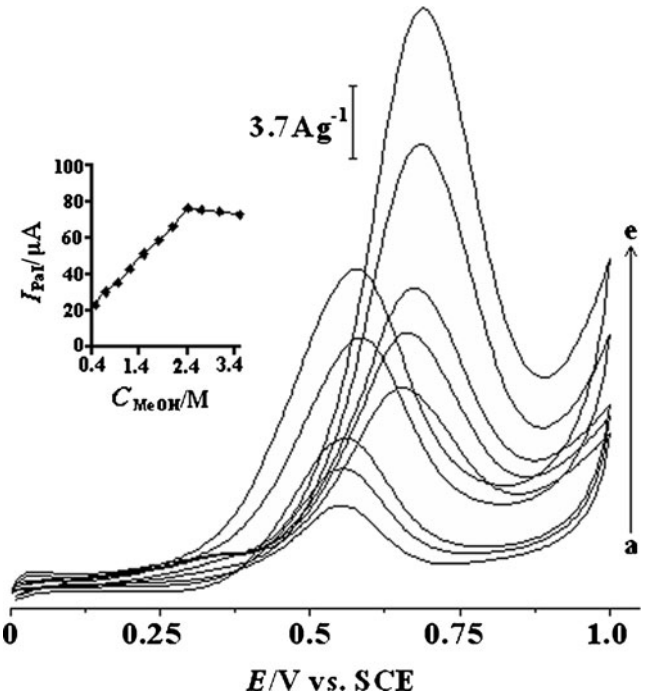

Fig. 8 Current–potential curves of the Pt/Nano-PDAN/MGCE in 0.5 M H_2SO_4 solution with different methanol concentrations at υ= 0.05 Vs^{-1}: *a* 0.47 M, *b* 0.70 M, *c* 0.93 M, *d* 1.8 M, and *e* 2.4 M. *Inset* plot of the anodic peak (*I*) current as a function of CH_3OH concentration

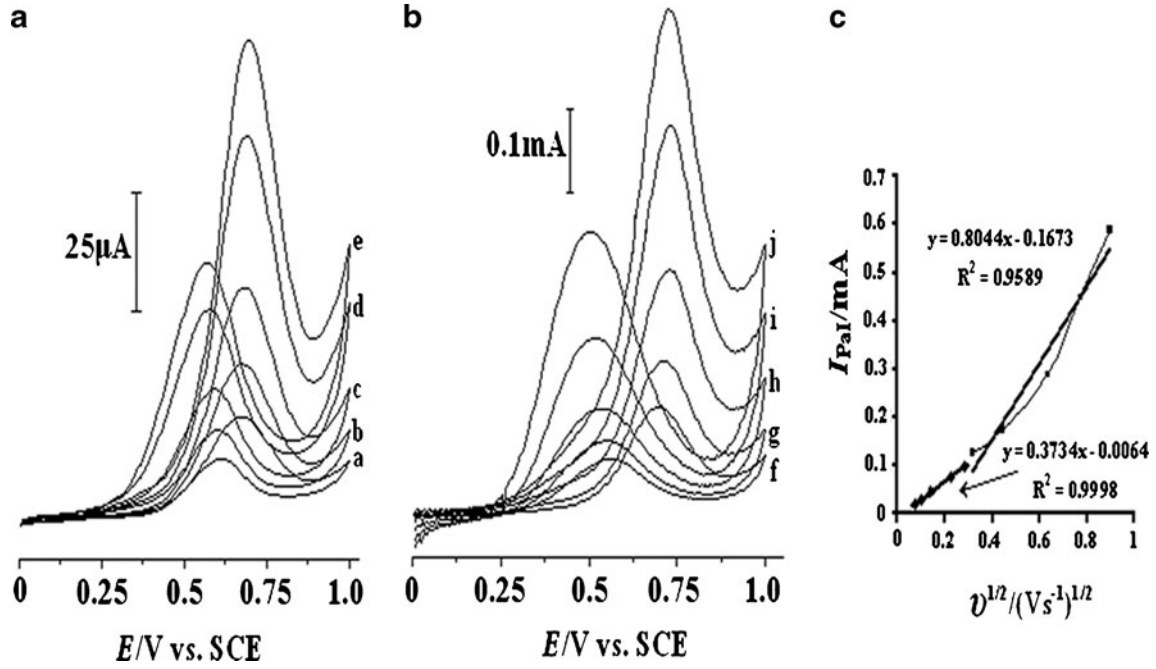

Fig. 9 Cyclic voltammograms of the Pt/Nano-PDAN/MGCE in 0.5 M H_2SO_4+2.4 M CH_3OH solutions; **a** at lower values of υ: *a* 0.005 Vs^{-1}, *b* 0.01 Vs^{-1}, *c* 0.02 Vs^{-1}, *d* 0.05 Vs^{-1}, and *e* 0.08 Vs^{-1} and **b** at higher values of υ: *f* 0.10 Vs^{-1}, *g* 0.20 Vs^{-1}, *h* 0.40 Vs^{-1}, *i* 0.60 Vs^{-1}, *j* 0.80 Vs^{-1}. **c** The dependency of the anodic peak (*I*) current obtained from **a** and **b** versus $\upsilon^{1/2}$

Electrocatalytic oxidation of methanol on the Pt/Nano-PDAN/MGCE

Figure 6 (dotted line) shows cyclic voltammogram of the Pt/Nano-PDAN/MGCE in 0.5 M H_2SO_4 in the presence of 2.4 M methanol after four cycles. The anodic current of methanol oxidation is started from about 0.2 V with low current, and by sweeping to the more positive potentials, the peak current density is highest at about 0.7 V (peak I). The oxidation peak current density decreases at more positive potential than region I due to the formation of Pt oxides. When the potential scan is reversed, reduction of Pt oxide to Pt can occur and clean Pt particle is available. The methanol oxidation takes place more easily onto clean Pt and therefore peak II appear. The height of this peak depends on the residue poisoning species on Pt surfaces.

For comparison, cyclic voltammogram of the Pt/MGCE towards the methanol oxidation was also shown in Fig. 5

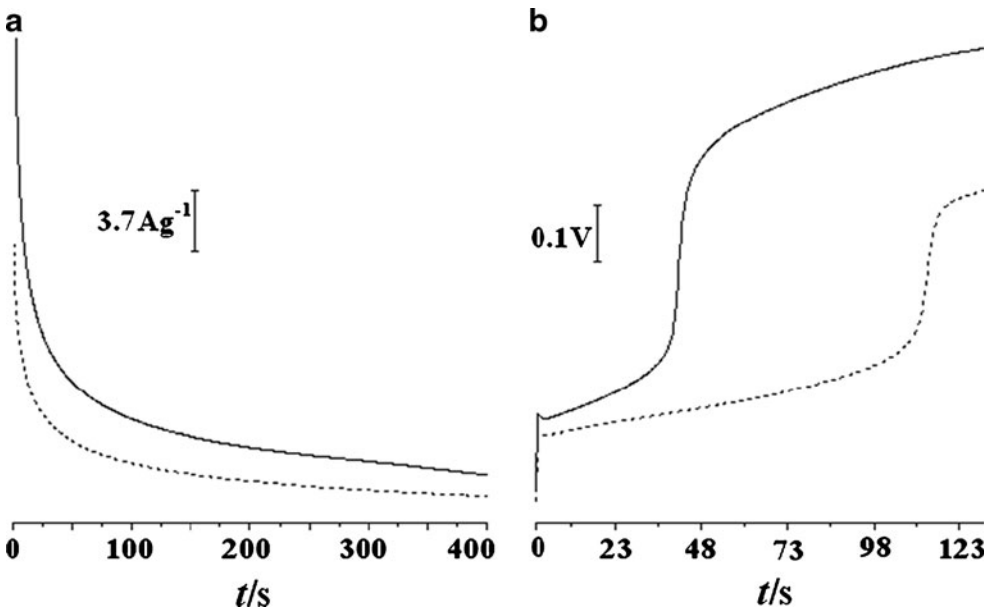

Fig. 10 **a** Chronoamperograms of the Pt/MGCE (*dotted line*) and Pt/Nano-PDAN/MGCE (*solid line*) in 2.4 M CH_3OH+ 0.5 M H_2SO_4 solution. Potential was applied from OCP (open circuit potential) to 0.7 V vs. SCE for 400 s. **b** Chronopotentiometric curves of the Pt/MGCE (*solid line*) and Pt/Nano-PDAN/MGCE (*dotted line*) at 7,400 mA g_{pt}^{-1}

(solid line). The current density (i.e., current normalized per true surface area/microamperes per square centimeter) difference between the voltammograms may be attributed to the larger surface area of the Pt particles in Nano-PDAN film. As can be seen in the figure, Pt/Nano-PDAN/MGCE yields higher current density than that of Pt/MGCE. These observations can clearly explain the role of PDAN on enhancement of the electrocatalytic oxidation current. Indeed, the Nano-PDAN is a proper bed for dispersion of Pt particles.

Effect of switching potentials on the methanol oxidation

In order to reveal the correlation between methanol oxidation and Pt oxide species, the effect of anodic limit of potential scanning on methanol oxidation at the Pt/Nano-PDAN/MGCE was studied (Fig. 7). As can be seen, the decrease of the upper limit potential causes: (a) an increment in the current of peak II and positive shift of its potential and (b) the currents ratio of two peaks I and II approaches to unity. Additionally, with increasing of scan upper limit, the peak I almost remain unchanged. These may be explained by preventing of the Pt oxide formation by lowering the upper limit potential cycling and consequently maintaining the electrode surface relatively clean.

The effect of methanol concentration

In order to evaluate the capacity of the Pt/Nano-PDAN/MGCE for methanol oxidation, the effect of concentration on the corresponding peak currents in 0.5 M H_2SO_4 solution was investigated (Fig. 8). It is clearly observed that the anodic peak currents increase with increasing of methanol concentration and drop afterwards at concentrations higher than 2.4 M. This effect may be attributed due to the saturation of Pt active sites and poisoning the electrode surface with adsorbed intermediates such as CO_{ads}.

Effect of potential sweep rates

The effect of potential sweep rates was studied on the electrocatalytic behavior of methanol onto Pt/Nano-PDAN/MGCE. As can be seen in Fig. 9, it is of interest to note that the curve exhibits a dual linear region. This phenomenon was also observed in the related literature [31, 32]. The possible explanation for this phenomenon is as follows: at higher potential scan rates, the reaction product accumulates in the vicinity of the electrode surface due to the higher reaction rate, and it will, in turn, decrease the adsorption of methanol molecules. In other words, the rate of methanol diffusion to the electrode surface can keep up with the lower potential scan rates. Additionally, since the rate of carbon dioxide production increases with increasing of potential scan rate, more electrolytes will be expelled from the pores of the electrode, thus decreasing the available surface of catalyst for electrochemical reaction.

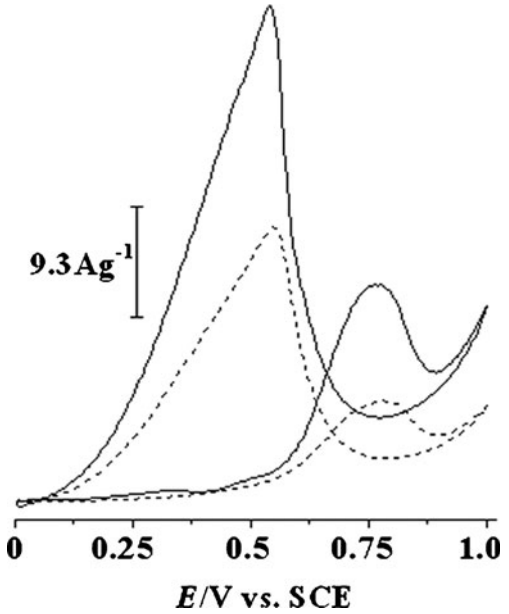

Fig. 11 Cyclic voltammograms of the Pt/Nano-PDAN/MGCE (*solid line*) and Pt/MGCE (*dotted line*) in 0.26 M formaldehyde+0.5 M H_2SO_4 solution at υ=0.05 Vs^{-1}

Comparison of stability

The stability of the Pt/Nano-PDAN/MGCE was examined by using cyclic voltammetry technique (figure not shown). The anodic peak current decreases gradually with potential cycling. In general, the loss of catalytic activity with successive scans of potential may result from the consumption of methanol during the potential scanning in cyclic voltammetry. It also perhaps due to poisoning and the structure changes of the Pt particles as a result of the potentials perturbation during the scanning in aqueous solutions, especially in the presence of organic compounds [33]. Another factor may be due to the diffusion process occurring between the electrode surface and bulk solution. With increasing of scan number, methanol diffuses gradually from bulk solution to the electrode surface. In H_2SO_4 solution,

Table 2 Comparison of the electrocatalytic oxidation peak potential of formaldehyde at the Pt/Nano-PDAN/MGCE with some polymeric-modified electrodes

Modified electrode	C_{HCHO}/M	E_p/V[a]	Reference
Pt/PAANI/MWNTs/GCE	0.50	0.72	[38]
Pt-Pd/PPy-CNT	0.50	0.60	[39]
Pt-PPy/CNT	0.50	0.63	[39]
Pt modified SWNT/PANI composite	0.50	0.62	[40]
Pt/Nano-PDAN/MGCE	0.26	0.75	This work

the electrode gets accumulated by CO_{ads} poison and hence the anodic current decreases.

For further evaluation of the catalytic activity and stability of the catalysts, chronoamperograms were recorded for methanol oxidation onto Pt/MGCE and Pt/Nano-PDAN/MGCE at the peak potential values (Fig. 10a). When the potential is fixed at peak potential values, due to the continuous oxidation of methanol on the catalyst surface, tenacious reaction intermediates such as CO_{ads} would begin to accumulate if the kinetics of the removal reaction could not keep pace with that of methanol oxidation. From the data, the higher oxidation current was obtained at the Pt/Nano-PDAN/MGCE. This suggests that the poisoning effect of generated intermediate species of methanol oxidation at the peak potentials is least on the modified electrode. Chronopotentiometry is another useful method to evaluate the stability and poisoning–tolerance abilities of the electrocatalysts for methanol oxidation. The potential increases with the polarization time and finally shifts to a higher potential value for oxygen evolution, indicating the poisoning of the catalysts [34]. It is evident from Fig. 10b that the potential increases with the reaction time and Pt/Nano-PDAN/MGCE can operate at a longer time than Pt/MGCE at the same mass activity. This result confirmed further that the Pt/Nano-PDAN/MGCE had better poisoning–tolerance ability than the other electrode.

Electrocatalytic oxidation of formaldehyde

The electrochemical oxidation of formaldehyde is important for full understanding of methanol oxidation in the development of fuel cell technology because it is an intermediate in methanol oxidation reaction. Figure 11 (solid line) shows a typical cyclic voltammogram of the Pt/Nano-PDAN/MGCE during the adsorption and oxidation of bulk formaldehyde. The mechanism of formaldehyde electrooxidation has been investigated in the relevance literature [35–38]. Briefly, in the cyclic voltammogram during the forward potential sweep, an oxidation peak can be observed at 0.75 V (attributed to the superposition of currents generated by the oxidation of CO_{ads} to CO_2 on the Pt surface, the intensively adsorbed species produced by the oxidation of formaldehyde and Pt). During the negative potential sweep, formaldehyde oxidation from a solution occurs as indicated by the presence of an intense anodic peak in the double layer region at 0.54 V. The obtained results showed that the electrocatalytic activity of the Pt/Nano-PDAN/MGCE towards formaldehyde oxidation was improved and higher than that of Pt/MGCE. The differences between electrochemical responses may be attributed to the large real surface area of the Pt particles dispersed into the Nano-PDAN film.

In comparison with some other polymeric modified electrodes, it seems clearly that Pt in the modified electrode can act as a comparable catalyst in formaldehyde oxidation (Table 2). Notably, the comparison of the anodic peak potential and stability for formaldehyde oxidation at the low cost modified electrode shows that this value is comparable with Pt-modified electrodes coated with different polymeric films. Also, the polymer film used in this work has a high mechanical stability. In addition, catalyst support material used in this work is an original matrix for dispersion of Pt catalyst.

Conclusion

1,5-diaminonaphthalene monomer can be electropolymerized onto GCE in sulfuric acid solution to give conductive polymeric film which presents high adherence to the electrode surface. High surface areas of Pt particles were obtained through preparing the Pt/Nano-PDAN composite film. The modified electrode showed higher catalytic activity towards oxidation of methanol and formaldehyde than that of Pt/MGCE. Furthermore, long-term stability of the modified electrodes was studied and it was found that Pt/Nano-PDAN/MGCE showed a higher stability towards methanol oxidation. On the other hand, the linear relationship between the anodic peak current and square rate of potential sweep rates can be observed. This implied that the electrooxidation of methanol at the surface of the modified electrode may be controlled by diffusion process.

References

1. Park JY, Scibioh MA, Kim SK, Kim HJ, Oh IH, Lee TG, Ha HY (2009) Int J Hydrogen Energy 34:2043–2051
2. Jung GB, Tu CH, Chi PH, Su A, Weng FB, Lin YT, Chiang YC, Lee CY, Yan WM (2009) J Solid State Electrochem 13:1455–1465
3. Khosravi M, Amini M (2010) Int J Hydrogen Energy 35:10527–10538
4. Wasmus S, Kuver A (1996) J Power Sources 58:239–242
5. Skowronski JM, Wazny A (2005) J Solid State Electrochem 9:890–899
6. Danaee I, Jafarian M, Forouzandeh F, Gobal F, Mahjani MG (2008) Int J Hydrogen Energy 33:4367–4376
7. El-Shafei AA (1999) J Electroanal Chem 471:89–95
8. Spataru T, Marcu M, Preda L, Osiceanu P, Moreno JMC, Spataru N (2011) J Solid State Electrochem 15:1149–1157
9. Said-Galiyev EE, Nikolaev AY, Levin EE, Lavrentyeva EK, Gallyamov MO, Polyakov SN, Tsirlina GA, Petrii OA, Khokhlov AR (2011) J Solid State Electrochem 15:623–633
10. Habibi B, Pournaghi-Azar MH (2010) J Solid State Electrochem 14:599–613
11. Adhikari A, Radhakrishnan S, Patil R (2009) Synth Met 159:1682–1688
12. Niu L, Li Q, Wei F, Wu S, Liu P, Cao X (2005) J Electroanal Chem 578:331–337
13. Razmi H, Habibi E (2009) J Solid State Electrochem 13:1897–1904
14. Jin GP, Peng X, Ding YF, Liu WQ, Ye JM (2009) J Solid State Electrochem 13:967–973
15. Hu ZA, Ren LJ, Feng XJ, Wang YP, Yang YY, Shi J, Mo LP, Lei ZQ (2007) Electrochem Commun 9:97–102
16. Yano J, Shiraga T, Kitani A (2008) J Solid State Electrochem 12:1179–1182

17. Selvaraj V, Alagar M, Hamerton I (2007) Appl Catal B Environ 73:172–179
18. Ojani R, Raoof JB, Hosseini SR (2008) Electrochim Acta 53:2402–2407
19. Ojani R, Raoof JB, Hosseini SR (2009) J Solid State Electrochem 13:1605–1611
20. Gloaguen F, Leger JM, Lamy C (1997) J Appl Electrochem 27:1052–1060
21. Laborde H, Léger JM, Lamy C (1994) J Appl Electrochem 24:219–226
22. Habibi B, Pournaghi-Azar MH (2010) Int J Hydrogen Energy 35:9318–9328
23. Abdelwahab AA, Lee HM, Shim YB (2009) Anal Chim Acta 650:247–253
24. Pham MC, Oulahyane M, Mostefai M, Chehimi MM (1998) Synth Met 93:89–96
25. Bard AJ, Faulkner LR (2001) Electrochemical methods, fundamentals and applications. Wiley, New York
26. Liu J, Mu S (1999) Synth Met 107:159–165
27. Cihaner A, Tirkes S, Monal A (2004) J Electroanal Chem 568:151–156
28. Herrasti P, Ocon P (1990) J Appl Electrochem 20:640–644
29. Cruz AGB, James LW, Rocco AM (2006) Synth Met 156:396–404
30. Kenneth AM, Zhou T (2002) J Electroanal Chem 521:53–60
31. He Z, Chen J, Liu D, Zhou H, Kuang Y (2004) Diam Relat Mater 13:1764–1770
32. Zhou W, Zhai C, Du Y, Xu J, Yang P (2009) Int J Hydrogen Energy 34:9316–9323
33. Parsons R, Vander Noot T (1988) J Electroanal Chem 257:9–45
34. Xu C, Shen PK (2004) Chem Commun 19:2238–2239
35. Villullas HM, Mattos-Costa FI, Nascente PAP, Bulhoes LOS (2004) Electrochim Acta 49:3909–3916
36. Stalnionis G, Tamasiunaite LT, Pautieniene V, Jusys Z (2004) J Solid State Electrochem 8:900–907
37. Nakabayashi S, Yagi I, Sugiyama N, Tamura K, Uosaki K (1997) Surf Sci 386:82–88
38. Jiang C, Chen H, Yu C, Zhang S, Liu B, Kong J (2009) Electrochim Acta 54:1134–1140
39. Selvaraj V, Alagar M, Kumar KS (2007) Appl Catal B Environ 75:129–138
40. Wang Z, Zhu Z, Shi J, Li H (2007) Appl Surf Sci 253:8811–8817